

Wind Tunnel Testing Of A Joined-wing Aircraft Model With Additive Manufactured Components

Teo, Zhen Wei; New, Tze How; Ong, Z. A.; Nagel, B.; Gollnick, V.; Pfeiffer, T.; Li, S.

2016

Teo, Z. W., New, T. H., Pfeiffer, T., Li, S., Ong, Z. A., Nagel, B., et al. (2016). Wind Tunnel Testing Of A Joined-wing Aircraft Model With Additive Manufactured Components. Proceedings of the 2nd International Conference on Progress in Additive Manufacturing (Pro-AM 2016), 170-175.

<https://hdl.handle.net/10356/84550>

© 2016 by Pro-AM 2016 Organizers. Published by Research Publishing, Singapore

Downloaded on 13 Mar 2024 16:10:58 SGT

WIND TUNNEL TESTING OF A JOINED-WING AIRCRAFT MODEL WITH ADDITIVE MANUFACTURED COMPONENTS

Z. W. TEO¹, T. H. NEW¹, T. PFEIFFER², S. LI¹, Z. A. ONG¹, B. NAGEL² and V. GOLLNICK²

¹*School of Mechanical and Aerospace Engineering, Nanyang Technological University
Singapore 639798, Singapore*

²*German Aerospace Center DLR, Institute of Air Transportation Systems
Hamburg 21079, Germany*

ABSTRACT: In this paper, the suitability of using additive manufacturing to fabricate aircraft test model components for use in wind tunnel testing will be reported. The purpose is to investigate the aerodynamic performance of a joined-wing aircraft model under subsonic flow conditions. The resulting test model wings are both complex and thin, and hence significant challenges surround the use of conventional machining due to vibrations from the cutting tools and non-trivial wing thinness. In contrast, additive manufacturing technique was able to overcome these fabrication issues, with a faster turnaround time, less material wastage and ease of design. However, surface finishing and cost issues associated with the additive manufactured components were observed during the study. In particular, significant deflections of the additive manufactured component were observed during testing, which could have explained discrepancies found between the experimental and numerical simulation results. Nonetheless, possible ways to correct these discrepancies will be described and discussed here.

KEYWORDS: Additive Manufacturing, Wind Tunnel Testing, Aerodynamics

INTRODUCTION

In the recent years, air traffic volume has experienced a sharp growth and this trend is expected to continue. Furthermore, with increasing attention paid towards pollution, there are higher pressures on airline operators to limit the impact on the environment by improving aircraft efficiencies. As such, there has been an uptick in interest in unconventional aircraft configurations to potentially improve the overall aerodynamic performance. One potential example is the joined-wing configuration studied here. The joined-wing concept, proposed by Wolkovitch (1986), involves the horizontal stabilizer sweeping forward to connect with the conventional main wing to form a diamond shape in both the frontal and planform view, as seen in Figure 1(a). This concept can be seen as an extension of Prandtl's work on biplanes and multi-planes (Prandtl, 1924). Frediani (2005) confirmed Prandtl's work on the "best wing", which gives the lowest induced drag, and calls it the PrandtlPlane. It is essentially similar to the joined-wing configuration, but with a connecting wing between the wing tips of the upper and lower wings, as seen in Figure 1(b). Much work has been done by Kroo (2001) and many others on the aerodynamic efficiency of non-planar wing systems and reducing the induced drag. However, it is not clear if the savings in the induced drag would outweigh the penalties incurred with the skin friction at cruise conditions. Hence, there lies a strong need for further wind tunnel testing to assess the aerodynamic characteristics of different joined-wing aircraft model designs. It should be noted nevertheless that joined-wing aircrafts typically have relatively thin wings and fabrication problems may arise when they are

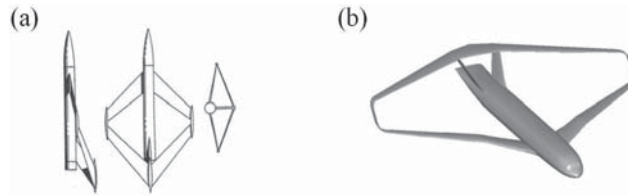


Figure 1. (a) Typical joined-wing configuration, Wolkovitch (1986) and (b) PrandtlPlane configuration with twin fins, Frediani (2005).

scaled down for wind tunnel testing. This paper will describe an experimental study in which these fabrication issues were overcome through additive manufacturing and how challenges arising from the use of more flexible additive manufactured components could be surmounted systematically.

EXPERIMENTAL SETUP AND PROCEDURES

Wind tunnel

Wind tunnel testing was conducted in a subsonic closed circuit wind tunnel with a test section size measuring $0.72\text{m (H)} \times 0.78\text{m (W)} \times 2\text{m (L)}$. It has a maximum operating velocity of 80m/s and a streamwise turbulence intensity level of 0.1% . During the testing, the test models were mounted on a sting balance which measured the aerodynamic forces and moments acting on it. The sting balance can measure up to 500N at 0.11% full-scale (FS) accuracy for the drag component and up to 600N at 0.14% FS accuracy for the lift component. Angle-of-attack (AOA) can be varied from -10° to 25° . The data was acquired by a National Instruments (NI) platform and channelled into an NI LabViewTM based software for monitoring and recording purposes. The overall data-acquisition system has a sampling rate of 47Hz , and 30 seconds of data were collected for each AOA.

Wind tunnel models

For the test models, the fuselages were machined out of 6061 aluminium alloy with a maximum surface roughness of $R_a 40$ microns. On the other hand, the joined-wings were fabricated through additive manufacturing with polyamide (PA) 2200, or nylon. Additive manufacturing was used as firstly, it had a shorter fabrication time and secondly, the complex design of the joined wings made it extremely difficult to fabricate with conventional machining due to the thinness of the wing, especially at the joints. The selected material was chosen after several factors such as the strength of the material, the surface finishing and the cost were taken into account. Test model surface finishing is important in wind tunnel testing as well, as it affects the location and extent of flow transitions, which in turn may impact upon the resulting aerodynamic behaviour, forces and moments. In order to ensure a satisfactory smooth finishing, the additive manufactured wings were also carefully sanded down using 2000 grit sandpaper. The strength of the additive manufacturing material used is important as well, since the components have to withstand the full extent of the aerodynamic forces throughout the entire study. The nylon material used has a reported flexural modulus of 1500MPa and flexural strength of 58MPa , which were deemed to be sufficiently robust for the wind tunnel experiments to be conducted.

Joined-wing aircraft test models

Three joined-wing test models were studied in the present investigation. The PP250 joined-wing design was provided by DLR, based on a previous study done by Bottoni and Scanu (2004), and was scaled down to fit into the wind tunnel test section for minimal wind tunnel wall interferences. For the sake of simplicity, the fuselage was modelled as a sharp-tipped ogive cylinder with a

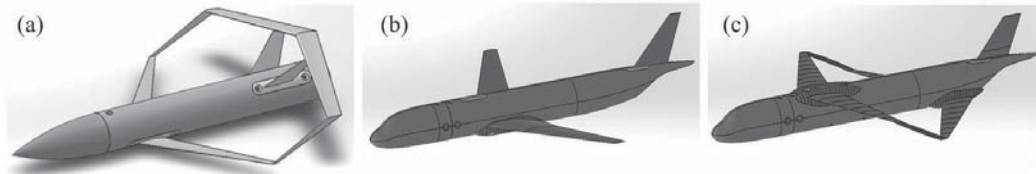


Figure 2. Physical geometries of (a) PP250, (b) D150 and (c) B150 joined-wing test models.

length of 0.528m, diameter of 0.06m and fineness ratio of 2.5. The span of the joined-wing was 0.372m and test velocities at 15m/s and 30m/s were used. Figure 2(a) illustrates the physical geometry of the complete PP250 test model. Note that while a higher fineness ratio could have led to improved lift-to-drag performances (Mayo, 1965), the physical geometry was constrained by the test section. Hence, a moderate value of 2.5 was used instead. The second D150 test model is representative of the Airbus A320 configuration and serves as a baseline case for benchmarking purposes. In this case, the fuselage was not simplified but was a scaled down version of the Airbus A320 fuselage such that it has a comparable fuselage diameter as the PP250 model for a more consistent comparison. The horizontal tails were not incorporated as the fuselage had to be fitted to the sting balance. The wingspan for the D150 model is 0.490m. Figure 2(b) shows the physical geometry of the D150 and the test velocities were from 15m/s to 60m/s. Lastly, the B150 test model has the same fuselage as the D150 configuration but with a different joined wing design. It was designed and optimized by DLR to have a similar planform area as the D150 test model wings. The purpose is to validate the vortex lattice codes used in the optimization procedures and confirm the additional benefits in the performance of the joined wing configuration over the baseline configuration. The wingspan for the B150 model is 0.380m and the test velocities were the same as the D150 configuration. Figure 2(c) shows its physical geometry.

Wing deflections and correction procedures

Significant wing deflections were observed during wind tunnel testing, due to the flexibility of the additive manufactured wings. To account for their impact upon the aerodynamic characteristics, a digital single-lens reflex (DSLR) camera was used to capture and quantify the deflections from two orientations - one from the side of the wind tunnel to quantify the deflections in the vertical axis, and another from within the wind tunnel to capture the curvature of the wings. For the former orientation, the camera captured the displacements of red dots marked on the leading-edge (LE) and trailing-edge (TE) of the wing tips. Images were captured when the wind tunnel was operational and non-operational for the sake of comparisons. The images were processed by a customized MatlabTM script to quantify the deflection and twist of the wing tips, such that the relative locations of the LE and TE could be determined. Alternatively, the procedures adopted by Shi et al. (2013) may also be used. For each image pair, the displacement vectors from the LE to TE were used to determine the average distances of the vectors and hence wing twist. Figure 3 shows the correction procedures for the D150 configuration pictorially. For the latter orientation, the DSLR camera was mounted onto a plate with pivot joints such that the camera height and angle can be adjusted. For the PP250 configuration, the plate was adjusted to match the AOA of the test model so that the camera faced the model normally. The white nylon wings provided good contrast against the black wind tunnel background, so no markers were needed. For D150 and B150 configurations, the camera was placed horizontally and level with the wings due to the wide range of AOAs studied. The lengths were then compensated through adopting the appropriate trigonometric relations. It should be noted that, for an even better contrast, the wing TE were coloured red for the D150 and red, green and yellow for the B150 to differentiate between the

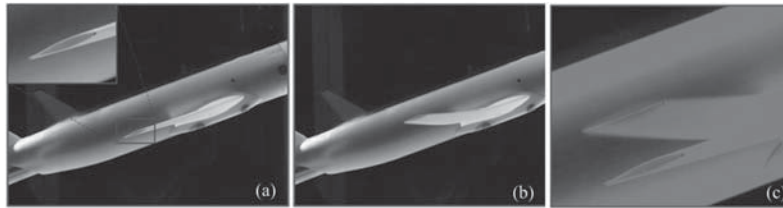


Figure 3. Determination of wing deflection and twist during the correction procedures.

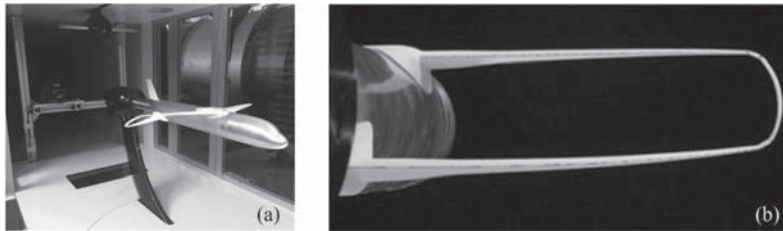


Figure 4. (a) Camera location in wind tunnel test section and (b) an image captured by the camera.

upper, lower and middle wings respectively. It was found that the images were slightly shifted upwards as the test velocity increased. Cross-correlation was used to shift the images so that they would coincide with each other. Figure 4 shows where the camera was located in the wind tunnel test section and the images captured for B150 test model.

NUMERICAL SIMULATIONS

In an earlier study reported by Teo et al. (2016), a comparison between the numerical simulation and wind tunnel results for the PP250 showed a slight discrepancy in terms of the predicted stall angle. The discrepancy could have been due to the wing deflections, for which it was not taken into account in the numerical simulations. Now that wing deflection data could be extracted from the present images, the deflected wing curvatures were incorporated into the geometry used for a new series of numerical simulations. Note that although all the three wing sections (i.e. upper wing, lower wing, as well as the middle wing connecting the upper and lower wings) were deflected, only the upper and lower wing curvatures were modelled. This was because contribution to both the lift and drag by the middle wing was insignificant compared to those by the upper and lower wings. To create the geometry and mesh for the numerical simulations, the lower wing root was assumed to originate at the same location as before and that the vertical tail remained non-deflected. Ten points separated at equal intervals along the upper and lower wings were chosen and used as guide points to create a smooth spline to model the wing curvatures. Figure 5 shows the difference between the original and reconstructed deflected wings, as well as a comparison with the actual physical wing. The mesh created for this new geometry was similar in count to that used by Teo et al. (2016) and all other conditions remained similar for a better comparison.

RESULTS AND DISCUSSIONS

For D150 configuration tested at 60m/s, Figure 6(a) shows that wing deflections estimated from the images according to the procedures laid out earlier show a trend that is grossly similar to the lift curve. This correlation should come as no surprise however, since wing deflections are expected to be closely related to the resulting aerodynamic forces. It is worthwhile to point out that

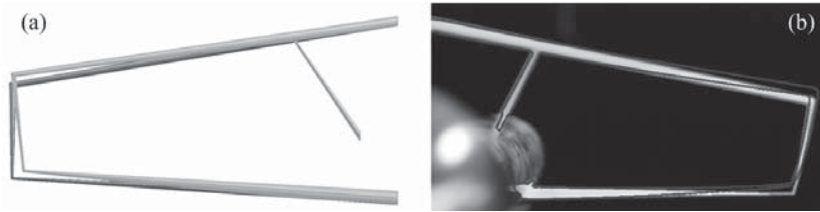


Figure 5. (a) Original and deflected wing drawings and (b) comparison with the actual wing.

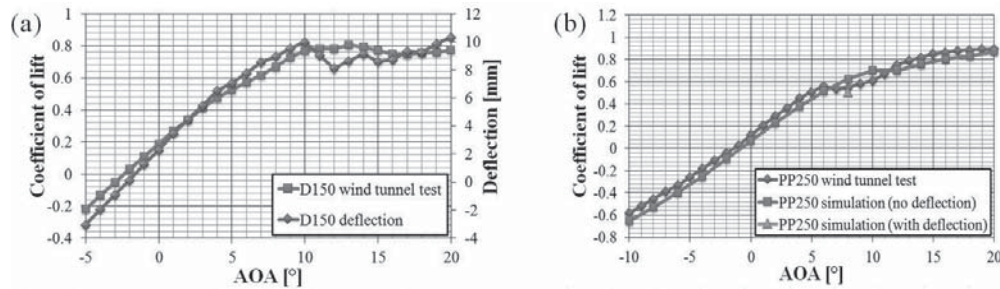


Figure 6. (a) Lift and deflection curves and (b) wind tunnel and numerical results comparison.

the deflection behaviour is not quite as predictable at higher AOAs. This is due to wing flutter at these higher AOAs, which in turn affects the accuracy in wing deflection determination. This was overcome somewhat by increasing the camera exposure time to estimate the mean wing deflections instead. In contrast, changes in the wing twist do not show any obvious correlation with the wing deflections or lift curve. In fact, wing twist was observed to fluctuate severely at higher AOAs due to wing flutter. However, wing twist was estimated to reach a maximum of 2° throughout the entire range of AOAs tested, which is negligible as compared to wing deflection.

As for the numerical simulations for the PP250 configuration, the incorporation of wing deflections into the geometry improves their accuracy. For instance, Figure 6(b) shows that the original discrepancy in the lift coefficient at 8° AOA has almost been eliminated. More importantly, it demonstrates that wing deflections have to be taken into account for experiments and numerical simulations involving aerodynamic characterizations. This is particularly the case here, where the joined-wing configurations are more complex and involve the use of thin additive manufactured wings. The present study also demonstrates that it is possible to compensate for the use of highly flexible additive manufactured wings in a systematic manner, and that their flexibility need not deter further implementations such as a wholly additively manufactured test model. With the systematic estimation of the wing deflections accounted for, future work involving the use of scalar visualizations [Lim et al. (2006), New and Tay (2006), New and Tsai (2007)] and particle-image velocimetry technique [New and Tsovolos (2009, 2011, 2012)] may be explored to look more closely into the vortex dynamics governing fore-wing and aft-wing flow interactions at different AOAs. Lastly, wings deflections at more AOAs may also be used to further validate the accuracy of the numerical simulations and wind tunnel experiments.

CONCLUSIONS

Wind tunnel testing of joined-wing aircraft test models with additive manufactured components was carried out. The tests revealed that nylon was sufficiently strong and flexible enough to

withstand the aerodynamic forces without failure. The surface finish was adequate and could be improved further by using fine grit sandpaper. Wing deflections were observed during testing and numerical simulations demonstrate that they could lead to discernible differences in the aerodynamic performance as compared to rigid models. This shows that additive manufacturing could be used to fabricate test models cheaply and quickly, so long wing deflections can be taken into account systematically and accurately. However, it should be highlighted that wing flutter at higher AOAs and velocities may make it harder to determine the true deflection accurately.

ACKNOWLEDGEMENTS

The authors gratefully acknowledge the support for this collaboration through a Helmholtz International Research Group grant from the Helmholtz Association (Germany). Numerical simulation and experimental design assistance provided by X. Gu at DLR and technical staff at Aerodynamics Laboratory, NTU respectively are greatly appreciated as well.

REFERENCES

- Bottoni, C., & Scanu, J. (2004). "Preliminary design of a 250 passenger PrandtlPlane aircraft", *University of Pisa*, Pisa, Italy, (unpublished).
- Frediani, A. (2005). "The Prandtl wing", Von Karman Institute Lecture Series: *Innovative Configurations and Advanced Concepts for Future Civil Transport Aircraft*.
- Kroo, I. (2001). "Drag due to lift: Concepts for predicting and reduction," *Annual Review of Fluid Mechanics*, 33, 587-617.
- Lim, T. T., New, T. H., & Luo, S. C. (2006). "Scaling of trajectories of elliptic jets in crossflow", *AIAA Journal*, 44(12), 3157–3160.
- Mayo, E. E. (1965). "Newtonian aerodynamics for tangent ogive bodies of revolution", NASA-TM-X-55235, X-671-65-244
- Nagel, B., Böhnke, D., Gollnick, V., Schmollgruber, P., Rizzi, A., La Rocca, G., & Alonso, J. J. (2012). "Communication in aircraft design: can we establish a common language?", *Proceedings of 28th International Congress of the Aeronautical Science*, Brisbane, Australia.
- New, T. H., & Tay, W. L. (2006). "Effects of cross-stream radial injections on a round jet", *Journal of Turbulence*, 7(N57), 1–20.
- New, T. H., & Tsai, H. M. (2007). "Experimental investigations on indeterminate-origin V- and A-notched jets", *AIAA Journal*, 45(4), 828–839.
- New, T. H., & Tsovolos, D. (2009). "Influence of nozzle sharpness on the flowfields of V-notched nozzle jets", *Physics of Fluids*, 21(8), 084107, 1–18.
- New, T. H., & Tsovolos, D. (2011). "On the vortical structures and behaviour of inclined elliptic jets", *European Journal of Mechanics - B/Fluids*, 30(4), 437–450.
- New, T. H., & Tsovolos, D. (2012). "On the flow characteristics of minor-plane inclined elliptic jets", *Experimental Thermal and Fluid Science*, 38, 94–106.
- Prandtl, L. (1924). "Induced drag of multiplanes," *NASA Technical Documents* NACA-TN-182.
- Shi, S., New, T. H., & Liu, Y. (2013). "Flapping dynamics of a low aspect-ratio energy-harvesting membrane immersed in a square cylinder wake", *Experimental Thermal and Fluid Science*, 46, 151–161.
- Teo, Z. W., New, T. H., Nagel, B., & Gollnick, V., (2016). "An experimental and numerical study on a small-scale joined-wing aircraft", *Proceedings of 54th AIAA Aerospace Sciences Meeting*, AIAA SciTech 2016.
- Wolkovitch, J. (1986). "The joined wing: An overview", *Journal of Aircraft*, 23(3), 161-178.